

Award Number: DAMD17-03-1-0532

TITLE: 4 Tesla MRI for Neurodegenerative Diseases

PRINCIPAL INVESTIGATOR: Michael W. Weiner, M.D.

CONTRACTING ORGANIZATION: Northern California Institute for Research &
Education
San Francisco, CA 94121

REPORT DATE: October 2005

TYPE OF REPORT: Annual

PREPARED FOR: U.S. Army Medical Research and Materiel Command
Fort Detrick, Maryland 21702-5012

DISTRIBUTION STATEMENT: Approved for Public Release;
Distribution Unlimited

The views, opinions and/or findings contained in this report are those of the author(s) and should not be construed as an official Department of the Army position, policy or decision unless so designated by other documentation.

REPORT DOCUMENTATION PAGE

Form Approved
OMB No. 0704-0188

Public reporting burden for this collection of information is estimated to average 1 hour per response, including the time for reviewing instructions, searching existing data sources, gathering and maintaining the data needed, and completing and reviewing this collection of information. Send comments regarding this burden estimate or any other aspect of this collection of information, including suggestions for reducing this burden to Department of Defense, Washington Headquarters Services, Directorate for Information Operations and Reports (0704-0188), 1215 Jefferson Davis Highway, Suite 1204, Arlington, VA 22202-4302. Respondents should be aware that notwithstanding any other provision of law, no person shall be subject to any penalty for failing to comply with a collection of information if it does not display a currently valid OMB control number. **PLEASE DO NOT RETURN YOUR FORM TO THE ABOVE ADDRESS.**

1. REPORT DATE 01-10-2005			2. REPORT TYPE Annual		3. DATES COVERED 30 Sep 2004 – 29 Sep 2005	
4. TITLE AND SUBTITLE 4 Tesla MRI for Neurodegenerative Diseases					5a. CONTRACT NUMBER	
					5b. GRANT NUMBER DAMD17-03-1-0532	
					5c. PROGRAM ELEMENT NUMBER	
6. AUTHOR(S) Michael W. Weiner, M.D.					5d. PROJECT NUMBER	
					5e. TASK NUMBER	
					5f. WORK UNIT NUMBER	
7. PERFORMING ORGANIZATION NAME(S) AND ADDRESS(ES) Northern California Institute for Research & Education San Francisco, CA 94121					8. PERFORMING ORGANIZATION REPORT NUMBER	
9. SPONSORING / MONITORING AGENCY NAME(S) AND ADDRESS(ES) U.S. Army Medical Research and Materiel Command Fort Detrick, Maryland 21702-5012						
10. SPONSOR/MONITOR'S ACRONYM(S)					11. SPONSOR/MONITOR'S REPORT NUMBER(S)	
13. SUPPLEMENTARY NOTES Original contains colored plates: ALL DTIC reproductions will be in black and white.						
14. ABSTRACT During the past year, nine research projects have used the 4Tesla magnet (for a total of 398 scans), and 55 developmental scans had been completed. Since the last progress report, we upgraded the shim currents which substantially improved the quality of imaging and spectroscopy, especially in problematic regions including the hippocampus and prefrontal lobe. The software platform was upgraded to the latest software version VA25 which provides better management and control of image processes. An "auto-align" software package was installed in order to improve reproducibility of image orientation and angulation using a template brain. Finally a whole body transmit coil and 7 KW transmitters have been ordered to improve uniformity of the B1-field and yield for arterial spinning. Our plans for the coming year are to test the performance of the auto align software on a large range of subjects with a broad range of brain abnormalities, and to complete the installation of the KW transmitters after the manufacturer performance tests are completed. The Center of Excellence funded six projects and five of these projects have the necessary approvals to begin work. We will continue the call for proposals and review and fund new innovative studies.						
15. SUBJECT TERMS Magnetic Resonance Imaging, Gulf War Syndrome, Alzheimer's Disease, Brain						
16. SECURITY CLASSIFICATION OF:				UU	18. NUMBER OF PAGES 14	19a. NAME OF RESPONSIBLE PERSON USAMRMC
a. REPORT U	b. ABSTRACT U	c. THIS PAGE U	19b. TELEPHONE NUMBER (include area code)			

Table of Contents

Cover	page 1
SF 298.....	page 2
Table of Contents	page 3
Introduction.....	page 4
Body, Key Research Accomplishments.....	page 4-14
Reportable Outcomes	page 14
Conclusions.....	page 14
References.....	N/A
Appendices.....	N/A

INTRODUCTION

Summary of Scanner use: During the past year nine projects have used the 4 Tesla magnet. In addition to scans completed for projects 55 developmental scans have been completed.

Project	# of completed scans
FAD (Four Tesla Assorted Diseases)	223
VAGW (V. A. Gulf War)	53
AFAR (American Foundation for Aging Research)	24
PCD (Prediction of Cognitive decline)	3
HI (HIV)	24
FT (Frontotemporal Dementia)	8
PT (PTSD)	5
SIV (Subcortical Ischemic Vascular Dementia)	7
FEP (Epilepsy)	39
PD (Parkinson's)	12

New upgrades since October 2004:

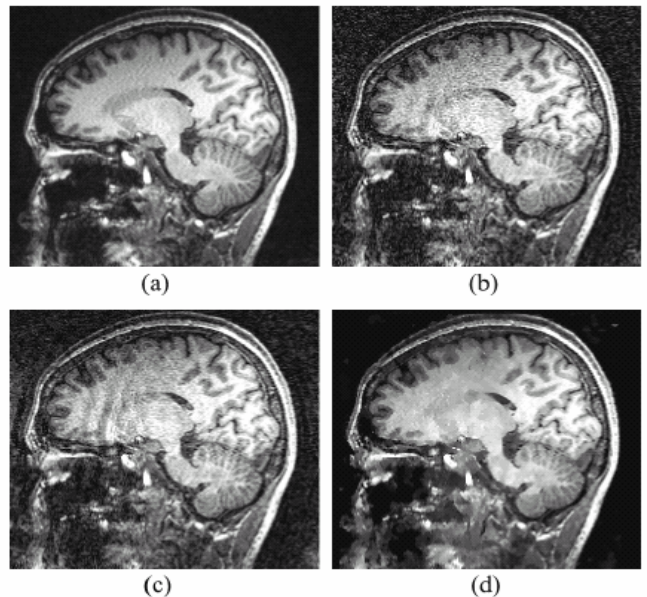
Since the last progress report, we upgraded the shim power supply from 5A to 10A per shim channel. The increase in shim currents substantially improved quality of imaging and spectroscopy, especially in problematic regions including the hippocampus and prefrontal lobe. In addition to hardware, the software platform of the system was upgraded to the latest software version VA25, which provides better management and control of disk space and synchronization of image processes. Finally, an “auto-align” software package was installed, which is designed to improve reproducibility of image orientation and angulation using a template brain. However, the performance of this program still needs to be tested for a larger range of subjects with a broad range of brain abnormalities, such as cortical atrophy and lesions. Finally, a whole body transmit coil and a 7 KW transmitters have been ordered in 2005 to improve uniformity of the B1-field and yield for arterial spin labeling. However, installation of these devices is being delayed because the manufacturer still needs to complete the final performance tests.

KEY RESEARCH ACCOMPLISHMENTS

The main research accomplishment over the past year was successful utilization of several key imaging techniques, especially high resolution structural MRI to study hippocampal subfields, volumetric arterial labeling perfusion MRI to measure brain function, and diffusion tensor imaging.

Advances in structural imaging

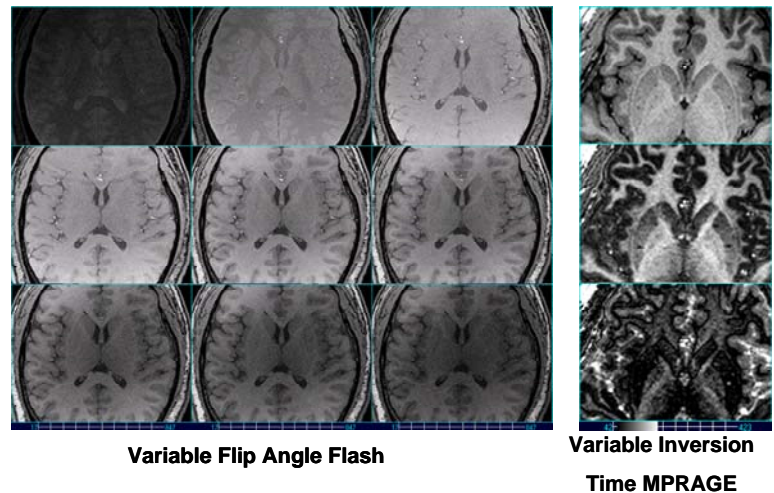
Improvements in high resolution structural MRI concerned primary accelerated acquisition utilizing parallel imaging methodology. Although the accelerated acquisition reduces SNR, the risk for image degradation, because of incidental head movement, is reduced because of shortening of the acquisition. Nonetheless, conventional parallel imaging methods can lead to substantial image artifacts when high acceleration factors are used. Bayesian methods with an appropriately chosen image prior offer a promising alternative; however,



previous methods with spatial priors assumed that intensities vary smoothly over the entire image, and therefore blur edges. We introduced an edge-preserving prior which instead assumes that intensities are piecewise smooth, and showed how to efficiently compute its Bayesian estimate. The estimation task is formulated as an optimization problem, which requires minimizing a non-convex objective function in a space with thousands of dimensions. As a result, traditional continuous minimization methods cannot be applied. Our optimization problem is closely related to some problems in computer vision for which discrete optimization methods have been developed in the last few years. We extended these algorithms, which are based on graph cuts, to address our optimization problem. Results of several parallel imaging experiments of brain under challenging conditions with high acceleration factors showed improvements over conventional SENSE methods. The figure shows (a) an unaccelerated image; (b) a factor 4 accelerated image with reconstruction using SENSE; (c) the same image using regularized SENSE reconstruction; and (d) the same image with the new reconstruction using graph cuts. The improvement with graph cuts in reducing aliasing artifacts as well as noise is clearly visible in (d).

Variable T1-weighted Imaging (VTI): A major limit of high resolution MRI are partial volume effects, where voxels contain variable amounts of gray matter, white matter and CSF, thus blurring tissue boundaries. Acquisition of VTI data could potentially eliminate partial volume effects by combining images with different contrasts. We have conducted initial experiments for VTI using FLASH with variable flip angles or MPRAGE with variable inversion-recovery times to test the dynamic range of T1 contrast changes and SNR. The currently implementation was performed with standard GRAPPA parallel imaging with an acceleration factor of 2, yielding 3D FLASH images in about 2:50 minutes and 3D MPRAGE images in 5:17 minutes. Representative VTI images are shown in Figure 1. Several important observations can be made from these preliminary data: First, this shows that a consistent change in T1 contrast can be achieved at 4T with both FLASH and MPRAGE. Although the dynamic range of T1 contrast changes is larger for MPRAGE than for FLASH, FLASH maybe more efficient in terms of sampling rate of multiple image frames per time. Second, effects from flip angle errors are visible in FLASH and are also impacting MPRAGE, emphasizing the importance for RF pulses with better immunity to B1-inhomogeneity and accounting for flip angle errors in data analysis and simulations. Third, SNR was sufficient even with acquisitions as short as 2 min and 5 min for FLASH and MPRAGE, respectively. This suggests that there is room for higher accelerations of at least another factor two, permitting acquisitions of more VTI frames that would improve estimation of partial volume effects.

Figure 1: Variable T1-weighted Images

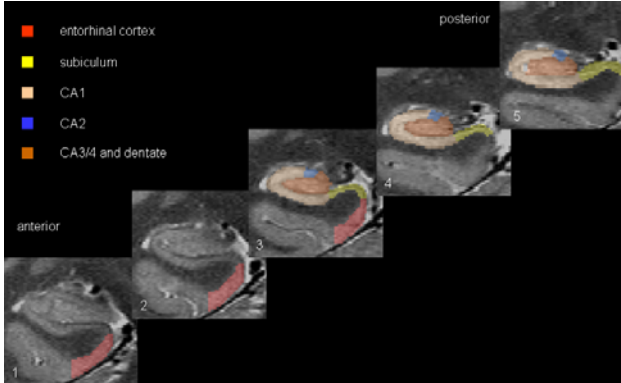


Several important observations can be made from these preliminary data: First, this shows that a consistent change in T1 contrast can be achieved at 4T with both FLASH and MPRAGE. Although the dynamic range of T1 contrast changes is larger for MPRAGE than for FLASH, FLASH maybe more efficient in terms of sampling rate of multiple image frames per time. Second, effects from flip angle errors are visible in FLASH and are also impacting MPRAGE, emphasizing the importance for RF pulses with better immunity to B1-inhomogeneity and accounting for flip angle errors in data analysis and simulations. Third, SNR was sufficient even with acquisitions as short as 2 min and 5 min for FLASH and MPRAGE, respectively. This suggests that there is room for higher accelerations of at least another factor two, permitting acquisitions of more VTI frames that would improve estimation of partial volume effects.

Measurement of Hippocampal Subfields

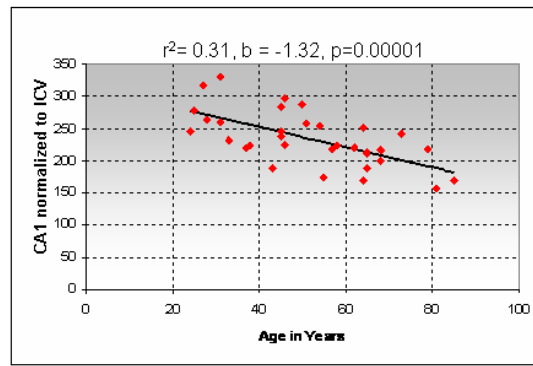
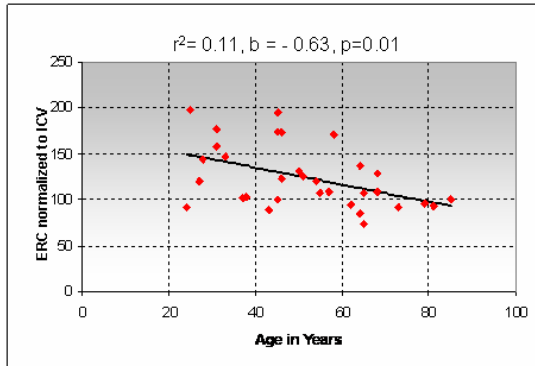
Recent advancements with high field MRI (3-4 Tesla), achieving increased gray/white matter contrast due to the increased signal sensitivity at high fields, additional magnetization transfer effects and T1 weighting, allow to acquire superb anatomical images of the brain at sub-millimeter resolution within a few minutes. This makes it possible to identify anatomical details which are not visible on images acquired on a 1.5 Tesla magnet, e.g. details of the internal structure of the hippocampal formation. The hippocampus is not a homogeneous structure

but divided into several subfields with distinctive histological characteristics: the subiculum, the four cornu ammonis sectors (CA1-4) and the dentate gyrus. Histological studies have shown that these subfields are differently affected by different diseases, e.g. Alzheimer Disease (AD) affects prominently the CA1 and the subiculum while leaving other subfields intact. Therefore, measuring hippocampal subfields might provide more diagnostic information than measuring the total hippocampal volume.



A high resolution T2 weighted imaging sequence (TR/TE: 3500/19 ms, echo train length 15, 18.6 ms echo spacing, 160° flip angle, 100% oversampling in ky direction, 0.4 x 0.5 mm in plane resolution, 2 mm slice thickness, 24 interleaved slices without gap, acquisition time 5:30 min) optimized for our 4T magnet by Drs. Stables and Schuff in our laboratory, was used to obtain high resolution images of the hippocampus. The details of the internal hippocampal structure visualized on these images were used to identify and measure CA1, CA2, CA3/4&dentate, entorhinal cortex (ERC) and the subiculum in 51 cognitively normal controls

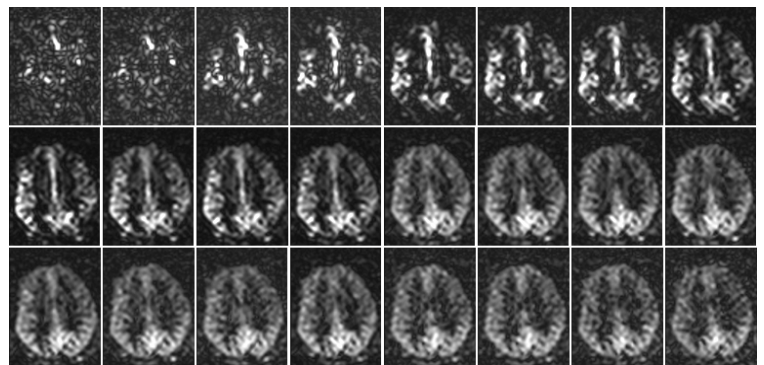
(aged 21-85, mean 52.1±17.8, m/f: 32/19). The subfield volumes were normalized to intracranial volume to account for differences in head size. The influence of age and gender on the different hippocampal subfields was tested using linear regression analyses. Significant negative age effects were found for ERC ($p > 0.01$) and CA1 ($p < 0.00001$). Based on these findings we concluded that measurements of hippocampal subfields might be helpful for differentiating healthy aging from pathological processes like AD.



Improvements in Perfusion.

3-D ASL-GRASE: With support of Dr. Feinberg, we implemented 3D ASL-GRASE at 4 Tesla and obtained preliminary results of serial 3D ASL perfusion imaging on a small number of healthy volunteers. Figure 2 depicts a time series of perfusion data from a healthy volunteer. Only one slice of 26 slices, covering the entire brain is shown. The acquisition of each 3D ASL frame took less than 34 seconds at a resolution of 4.5 x 4.5 x 4.5 mm. The image series shown in Figure 2 was acquired with increasing post-labeling delays from 200ms to 2500ms in steps of 100ms. The spatial dispersion in the arrival of the ASL signal can clearly be seen in the

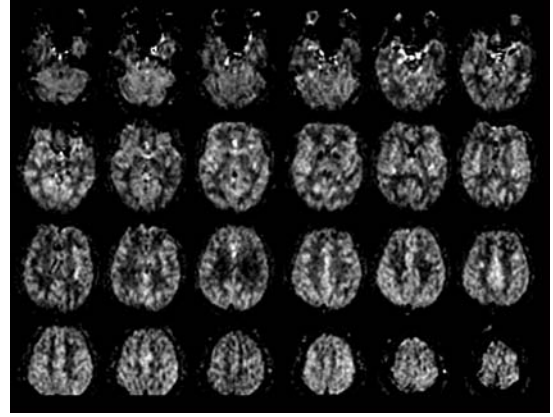
Figure 2: Perfusion Time Series from 3D ASL-GRASE



upper row of Figure 2. Also clearly visible from Figure 4 is the progressive disappearance of the arterial component of the ASL signal, as water diffuses into the brain. Moreover, this particular subject showed a left/right and anterior/posterior asymmetry of perfusion, as seen in the middle row of Figure 2. The data show that serial ASL measurements to quantify cerebral flow are possible within a few minutes at 4T using 3D ASL GRASE.

Continuous Arterial Spin Labeling: As an alternative to 3D GRASE, a 2D ASL sequence was also installed using continuous ASL, which generally yields more labeling than pulsed techniques. This sequence is currently used in our standard MRI protocol. The images in Fig. 3 show representative perfusion images that were obtained using this sequence (sequence was provided by courtesy of Drs. Wang and Detre of University of Pennsylvania). Acquisition of 24 slices, each 3mm thick with $2.4 \times 2.4\text{mm}^2$ resolution and 120 scan averages took about 8 minutes. Sensitivity of this sequence is very promising to obtain perfusion data even in white matter, which yields usually a much weaker perfusion signal than in gray matter.

Figure 3: 4Tesla Continuous ALS -MRI



Improved Methods to Measure Perfusion in White Matter at 4T

We further investigated measurements of CBF in white matter at 4T. Specifically, we compared the ability of EPI to measure CBF of white matter with that of Turbo-FLASH (TFL). We also incorporated an improved pulsed arterial spin labeling design, to measure CBF in WM. We found that CBF of WM remained largely constant for a wide range of postlabeling delays, which is likely explained by a large dispersion of time-to-arrival in WM for labeled spins. An interesting observation was that TFL-systematically yielded lower CBF values in GM and WM than EPI. Furthermore, in GM this difference seemed to become more prominent with increasing postlabeling delays. A likely explanation for this is that CBF measurements based on TFL are less contaminated by vascular contributions than EPI, representing more accurately the signal component that is due to perfusion. In conclusion, CBF measurements in WM are feasible at 4T and should be conducted using TFL to obtain an accurate representation of the signal that is due to perfusion.

Improved Methods for Arterial Spin Labeling

Recently, pseudo-continuous flow driven spin inversion based on repeated shallow flip angle radiofrequency (RF) pulses was proposed for arterial spin labeling (ASL) perfusion MRI at higher magnetic fields, but the limits of the pulse were not completely understood.

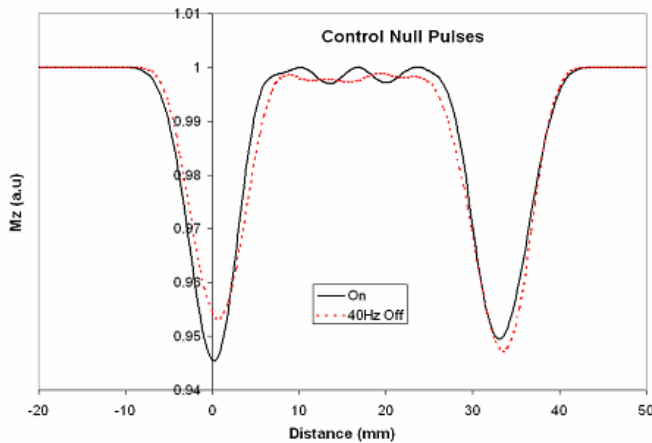


Fig. 4. Simulation of the magnetization (Mz) of spins flowing at a velocity of 40 cm/sec after applying the proposed null pulse. Both on- (black) and 40 Hz off-resonance (red) conditions are shown.

Although the null pulse design worked well for static spins, our simulations with MATPULSE showed that the performance quickly degraded for flowing spins. We found the flow of the spins created a mismatch (phase error) between the phase of the spins and their position. Thus, a subsequent pulse in the series did not entirely undo the rotation of the previous pulse, producing a cumulative tipping over a pulse series. We solved this problem by applying the null pulses at an off resonance frequency of 200 Hz, which destroyed the cumulative effect of the tipping, resulting in almost no net tipping as the spines traversed the slice. Simulations with MATPULSE show (see Fig. 4) that the null pulse applied

off resonance produced almost no net magnetization over a wide range of flow velocities, obviously the null pulse is improved by destroying the accumulation of phase errors. Note also in Fig. 4 the induced transverse magnetization is less than 6%. The improved understanding of the sequence should enable a rational approach to extending the range of flow velocities over which the pulse sequence is effective, as well as minimizing RF power deposition of the sequence while still maintaining a reasonable range of flow velocities over which both the inversion and null sequences perform. The significance of this work is that this pseudo-continuous pulse should be especially useful for ASL at high magnetic fields, because the pulse has a low power deposition yet provides a high yield for spin labeling.

Regional Decline of Brain cerebral Blood Flow in Healthy Aging by High-Field Arterial Spin Labeling

Background:

We reported previously weak inverse relationship between brain perfusion and age using Arterial Spinning labeling (ASL) MRI. However, sensitivity to measure perfusion was limited due to poor signal-to-noise of ASL at 1.5T. Since ASL sensitivity increases substantially with higher magnetic fields, and more brain regions can be covered because of longer T1 time, we performed this ASL study at 4T on aging.

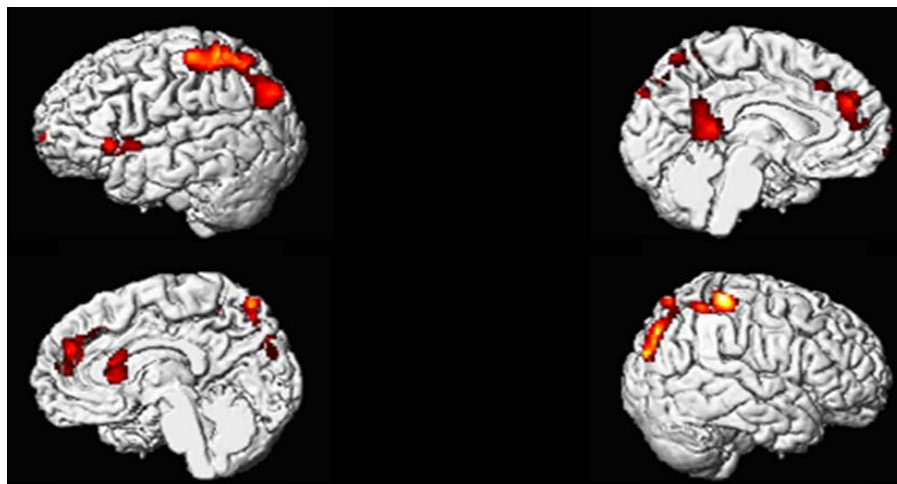
Objectives: 1) to explore if ASL-MRI at 4T detects a regional pattern of diminished cerebral blood flow (CBF) with age. 2) To explore if CBF is different between men and women; 3) to test the concordance and dissociation of CBF decline and GM volume loss with aging.

Methods

Thirty-eight healthy volunteers from 23 to 85 years old (13 women and 25 men) were included in this 4T MRI study. Perfusion weighted images (16 slices with $3.75 \times 3.75 \times 6.2$ mm³ resolution) were acquired using the amplitude-modulated continuous ASL in addition to T1- and T2-weighted structural images. CBF was calculated based on a single compartment model. Aging effects on CBF and GM decline were tested voxel-wise using Statistical Parametric Mapping (SPM2). In addition, the concordance and dissociation between CBF decline and GM volume loss with age was tested by a permutation test.

Results: There was a significantly inverse relationship ($p < 0.001$) between age and CBF in bilateral anterior cingulate, precuneus and superior parietal regions, and left posterior cingulate and superior temporal regions. However, there was no different CBF between men and women. A significantly inverse relationship ($p < 0.001$) between age and GM volume loss was found in bilateral frontal, temporal, parietal and occipital regions and basic ganglia. The concordance of CBF decline and GM volume loss with age was found in bilateral superior temporal regions, and right superior parietal regions. However, there was no dissociation between CBF decline and GM volume loss with age in any brain regions.

Discussion: We observed a regional pattern of age-related decline in brain perfusion using ASL-MRI by 4T, consistent with imaging studies using SPECT and PET. The combination of perfusion decline and GM volume loss may be useful in differentiate normal aging from other pathologies such as Alzheimer's disease.



Tractography-based and Voxel-Based studies of White Matter Changes in Normal Aging Using Diffusion Tensor Imaging on 4T

Introduction

Diffusion tensor imaging has been used to investigate white matter structural integrity in normal ageing. Numbers of studies using region of interest (ROI) approaches have lead to debate about the regional specificity of white matter decline in aging, in particular that the frontal lobes are preferentially affected. Recently, some voxel-based statistical analyses also showed an agreement with ROI studies that white matter damage across the aging brain particularly distributed in the frontal brain. However, white matter changes along specific fiber bundles were not been fully investigated. In this study, we used tractography-based analysis of fractional anisotropy (FA) on two white matter fiber tracts: the corpus callosum (CC) and the cingulum (Cg), by divided sub-regions. The purpose is to investigate the extent of these white matter pathways affected in the aging process. In addition, voxel-based analysis of the whole brain FA were performed to investigate the distribution of age-related FA reduction in whole brain, and whether these two methods lead to different conclusions of normal aging on same DTI data.

Methods

MRI data acquisition and preliminary analysis: Fifty-one healthy subjects (29 male, 22 female; Age 22-79 yrs) were involved in the study. DTI was performed on a 4.0 Tesla scanner. DTI were using single-shot EPI sequence (TR/TE=6000/77ms, voxel size: $2 \times 2 \times 3 \text{mm}^3$, 40 contiguous slices, $b=0$, 800s/mm^2 , and 6 directions, 4 averages). DTI post-processing was using Diffusion Tensor Visualizer (dTV) software (<http://www.ut-radiology.umin.jp/people/masutani/dTV.htm>) to generate FA, MD, and color-coded maps. These images were interpolated to $2 \times 2 \times 2 \text{mm}^3$ resolution for fiber tracking.

Tractography-based analysis: Callosal fiber and cingulum fiber tracking were using FACT method, FA threshold were at 0.3 for CC fibers and 0.18 for Cg fibers, stop angles were at $30\text{-}40^\circ$. The tracked fibers were displayed as fiber maps; together with FA maps were re-orientated to a standard position—with the bottom of genu and splenium along the same level on mid-sagittal view. These re-orientated maps were then transferred to MRICro (<http://www.sph.sc.edu/comd/rorden/mricro.html>) for sub-region analysis: for CC fibers, sub-regions were selected from 3 mid-sagittal slices, divided averagely by 5, from anterior to posterior (CC1-CC5) (Figure 5). For Cg fibers, sub-regions were divided as anterior (aCg), posterior (pCg), and temporal (tCg) regions along the fiber (Figure 6). Mean FA values for each sub-region were measured by plotting out pixels of these fibers and overlaying on the FA maps.

Voxel-based analysis: An average parametric FA template were created by SPM2, FA map for each subject was normalized to the FA template and re-sampled to 2.0mm^3 voxels, then smoothed (10mm^3 FWHM). An absolute threshold of $\text{FA} > 0.2$ was used to eliminate voxels in ventricle and grey matter. Statistical analysis was performed using a linear correlation model, with multiple comparisons correction using a family wise error at $p < 0.05$ corrected for peak height.

Results

Tractography-based analysis: Table 1 summarized the statistical results of FA against with age from the CC fibers and Cg fibers. With increasing age, FA significantly decreased in CC1, CC2, while remaining stable in CC4 and CC5. FA also significantly decreased in bilateral aCg, right pCg, but remained stable in bilateral temporal Cg. In addition, a left > right asymmetry of FA values were found in the anterior to posterior Cg, but the tCg were symmetric.

Voxel-based analysis: FA revealed extensive negatively correlated with age in peri-callosal white matter of frontal, parietal, occipital, and temporal lobes, and genu of CC, posterior limb of internal capsule. Overall, age-related FA reduction was more significant in the frontal lobes than in the rest of the brain (Figure 7).

Discussion

Tractography results suggest that FA substantially reduced with increasing of age in anterior CC fibers and anterior Cg fibers, whereas the splenium of CC and temporal branch of the Cg are spared. Agree with these results, Voxel-based analysis also showed an age-related FA reduction, anterior frontal lobes being particularly affected. This is in keeping with results from other studies. Measuring of mean FA voxels within fibers could explain changes of integrity along certain bundled fibers, if well performed tractography. SPM analysis, however, had lower statistical significance than tractography-based study, seemed to over-estimate the extant of FA changes, is highly dependent on spatial normalizations. Both methods did not show age-related FA decline in the temporal Cg bundles, it remains to be investigated whether cognitive functions affect this area.

Figure 5. Sub-region divisions for the CC fiber

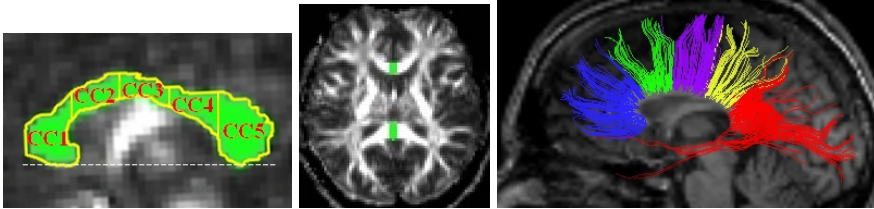


Figure 6. Sub-region divisions for the Cg fiber

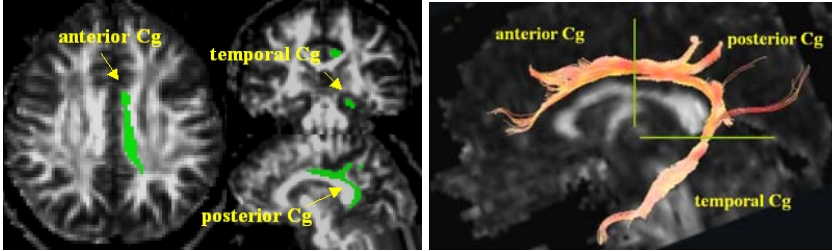


Figure 7. SPM significant clusters of FA against with age

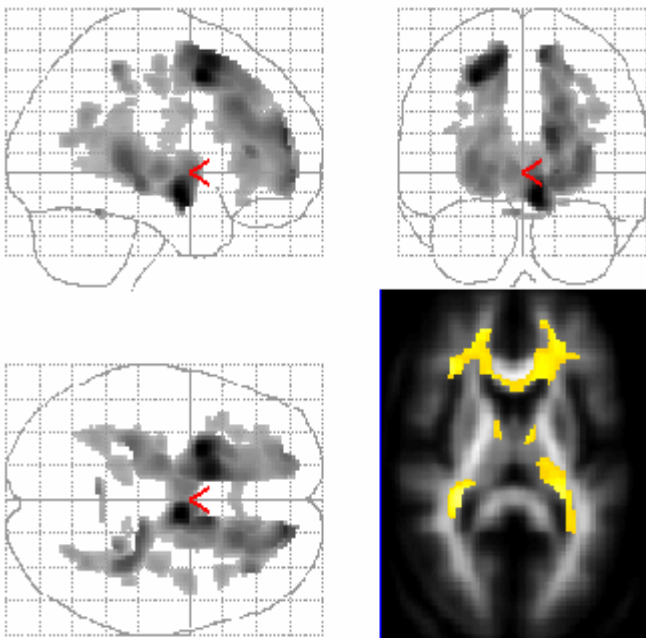


Table 1. Age-effects on FA

Sub-regions	FA coefficients	P values
CC 1	-0.0016	<0.0001
CC 2	-0.0017	0.0007
CC 3	-0.0011	0.07
CC 4	-0.0013	0.11
CC 5	-0.0005	0.2
left tCg	-0.0002	0.75
right tCg	-0.0002	0.48
left pCg	-0.0005	0.17
right pCg	-0.0007	0.01
left aCg	-0.0008	0.01
right aCg	-0.0008	0.04

Susceptibility weighted imaging

Since March 2005, we have been investigating the use of a novel imaging method, SWI, to evaluate brain tissue iron at 4T. SWI images emphasize local distortions in the magnetic field caused by iron in tissue and in venous blood. While most applications of SWI have been in venography, we are interested in extending its use to evaluate the levels of iron deposits in brain tissue. Increased brain iron deposits are found in a number of neurodegenerative diseases, in particular Alzheimer's disease (AD) and Parkinson's disease (PD), therefore our goal is to determine whether SWI can be helpful in the early diagnosis of these conditions.

After obtaining the SWI sequence through a research collaboration, we optimized its acquisition for the evaluation of tissue iron at 4T. In particular, we maximized contrast for imaging the basal ganglia, a group of nuclei in the brain which are severely affected in PD. We have since imaged 12 patients with PD or similar conditions, as well as a large number of age-matched controls. To analyze the data, our next step will be to warp the images onto a common atlas so that differences between the SWI images of PD's and controls can be directly compared.

Echoplanar MRSI

Development of volumetric echo-planar spectroscopic imaging (3D EPSI) is currently aimed at reducing the minimum acquisition time by utilizing advanced sampling strategies that offer enhanced sampling efficiency. One approach that is under consideration is termed body-centered cubic (bcc) sampling and takes advantage of a principle similar to that of "cubic close packing", the most efficient strategy for arranging spherical objects in 3D space. It was determined that, using bcc sampling for 3D EPSI and assuming that signal is band-limited in image space to an ellipsoidal region, a maximum reduction in acquisition time by almost a factor of 2 could be achieved. A fast reconstruction algorithm for bcc sampling was implemented, and data simulations were carried out to investigate the behavior of 3D EPSI data sampled with the bcc approach. Future development will involve integration of the bcc sampling approach into the 3D EPSI pulse sequence and evaluation of phantom test data with respect to spatial resolution, signal-to-noise ratio, and spectral quality.

A second approach to reducing the minimum acquisition time, termed blipped phase-encoding, takes advantage of some redundancy in the gradient echo train used in the 3D EPSI acquisition. By applying short phase-encoding pulses ("blips") within the echo train, data are effectively encoded with information corresponding to two different locations in the phase-encoded dimension. This allows elimination of every other phase-encoding step, and thus of every other sequence repetition, and leads to a reduction in minimum acquisition time by a

factor of 2. A preliminary version of this approach was implemented on the 4 Tesla MRI system. Metabolite images obtained from a normal volunteer are shown below. Future work will include improved acquisition and reconstruction strategies to reduce the residual ghost artifacts visible in the images (Fig. 8, top row) and to improve spatial resolution.

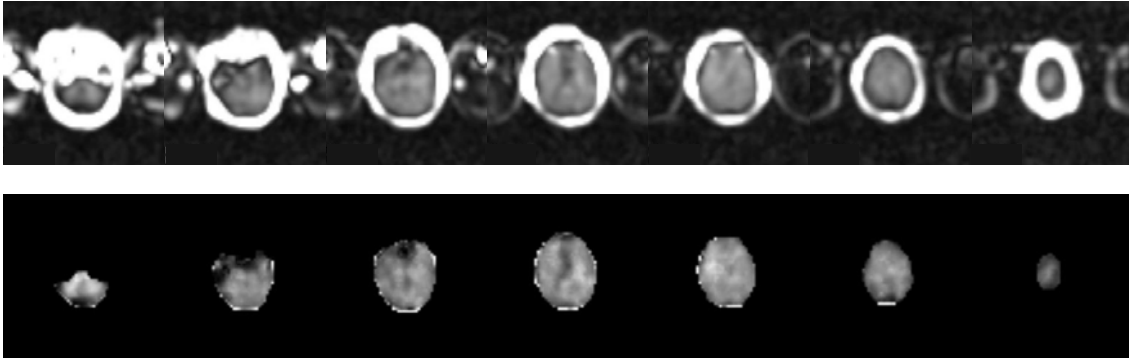
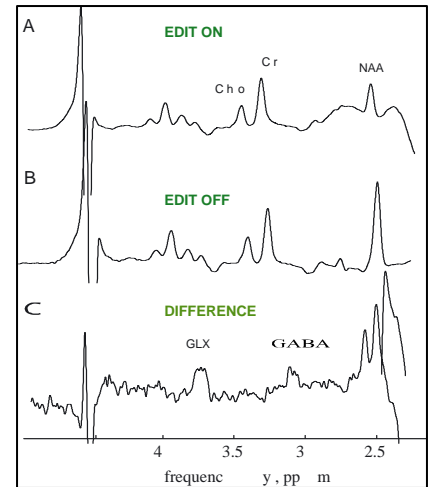


Fig. 8: 3D EPSI images showing the distribution of N-acetyl-aspartate (NAA) in the brain of one healthy volunteer obtained with blipped phase-encoding. Top row: Images obtained by spectral integration of the NAA signal at 2.01 ppm; bottom row: Images obtained by spectral fitting of the same data.

Single voxel ^1H MR Spectroscopy (SVS)

SVS is a powerful tool for *in vivo* detection of various metabolites in the human brain. One of the most important neurotransmitters in the human brain is γ -aminobutyric acid (GABA), which is implicated in an altered GABAergic function in various human disorders, including epilepsy, schizophrenia and substance abuse. Due to significant spectral overlap between the resonances even at high field, observation of GABA requires a special experiment, such as spectral editing. In the course of last year, PRESS-localized J-difference experiment was developed on Siemens/Bruker 4 Tesla system. In addition, computer simulations were carried out to optimize the acquisition and quantification parameters. Figure below demonstrates the results of the editing experiment at 4 Tesla, where the bottom spectrum (C) (which is a difference of spectra A and B) contains GABA signal that can be unambiguously quantified.



4T MR Spectroscopy GABA Studies in Alcoholism

Efforts were aimed at finding the most optimal protocol for quantitative clinical GABA measurements in different cortical brain regions. Together with Dr. Lana Kaiser, we implemented and tested various versions of a PRESS-localized J-difference experiment on the Siemens/Bruker 4 Tesla system. We tested in both phantoms and human controls the performance of different editing pulses, their optimal frequency positions, bandwidths and profiles, spoiler gradients and phase cycling, approaches to suppressing co-edited macromolecular contributions and lipid signal, and efficient water suppression schemes. Computer simulations aided in optimizing the acquisition and quantification parameters. Protocols were also set up in MATLAB to process the spectral data and to quantify it by using FTT software used in this lab for other spectral quantitation projects.

This last year, a total of 16 such development studies were performed on 6 healthy volunteers recruited from the community and lab personnel and on 10 recovering alcoholics enrolled in a NIH funded study on the effects of

chronic drinking and abstinence on the brain (PI: Meyerhoff). All studies aimed at acquiring GABA spectra with the phased-array head coil in parieto-occipital cortex (40x20x20mm³), the later studies placed volumes of interest also on medial prefrontal cortex (including the anterior cingulate cortex, 30x25x20mm³), and lateral temporal cortex (20x40x20mm³).

The studies clarified the best experimental conditions for clinical GABA measurements and showed that good and quantifiable GABA spectra can be obtained from the parieto-occipital cortex and the medial prefrontal cortex. We do not have enough experience yet with data acquisition in temporal cortex.

Proton MRS in Primary HIV Infection.

This research is performed in collaboration with Dr. Serena Spudich, a neurologist SF General Hospital/UCSF, who has obtained a NIH K23 Career Development Award and is being mentored by Dr. Meyerhoff in neuroimaging of HIV infection. The central hypothesis of this HIV study is that early neuroinvasion by HIV involves viral trafficking in the setting of host immune activation and allows establishment of persistent and compartmentalized CNS infection.

Thus, the primary goal of this proposal will be to longitudinally define CNS host responses and viral features during early exposure to HIV through serial clinical, CSF, and high magnetic field (4 Tesla) MRI and MRS analyses. Brain MRI/MRS will measure concentrations, spectral profiles, and regional and temporal patterns of cerebral metabolites, thus providing a sensitive in vivo method to measure cell-specific and inflammatory changes. Alterations in metabolites such as choline, myoinositol, and n-acetylaspartate detect gliosis, cell turnover, and neuronal injury/loss. New high-field MRS allows measurement of glutamate, an important potential mediator of neurotoxicity in AIDS. The research aims at providing an 'experimental' background for study of the dynamics of viral trafficking, host immune responses, and CNS injury and repair associated with substantial changes in viral burden. To this end, study of primary infection (within the prior 6 months) will be complemented by parallel study of participants undergoing interruption and initiation of antiretroviral therapy.

To this end we implemented a longitudinal MRI/MRS protocol on the 4T that obtains standard structural MRIs and single-volume PRESS data from the frontal WM, the basal ganglia, the anterior cingulate cortex, and more recently the medial posterior cortex. DTI data is obtained from the entire brain if time allows. Since December 2005, we enrolled 8 HIV+ individuals with primary HIV infection, who individually were studied up to 3 times within 10 weeks using our phased-array head coil. Spectral quality is checked routinely immediately after data acquisition by performing basic spectral processing in MATLAB. The data is being prepared for spectral fitting using FTT software.

Predicting HAD using Monocyte Profiling and Neuroimaging.

This research is performed in collaboration with Dr. Lynn Pulliam, SF VA Medical Center/UCSF. The overall hypothesis is that patients at risk for HIV-associated dementia (HAD) have a distinct monocyte gene expression profile that is related to /reflected in neurocognitive deficits and MR-observable structural and metabolite abnormalities.

Gene expression profiles are correlated with results of neuropsychological testing and quantitative volumetric MRI and of quantitative MRS to develop a better understanding of risk factors associated with observable brain injury in HIV-1 patients on HAART. Recent findings show that MRI and MRS can detect CNS involvement early in asymptomatic patients. One of the specific aims is to identify a monocyte gene expression profile from HIV-1-infected VA veterans that correlates with injury to specific brain structures and metabolites measured by MRI and MRSI, respectively. Risk factors, HIV-1 high viral load and APOE genotype, will be assessed as potential modifiers. A supplemental aim is to associate HIV-1-related changes in monocyte gene expression, neuroimaging and neuropsychological testing with genetic variation identified by single nucleotide polymorphisms analysis.

To this end we implemented a longitudinal MRI/MRS protocol on the 4T that is almost identical to that for the HIV study described above. Since October 2005, we enrolled 24 HIV+ individuals with high and low viral loads, who were studied once with our phased-array head coil. Spectral quality is checked routinely immediately after data acquisition by performing basic spectral processing in MATLAB. The data is being prepared for spectral fitting using FITT software.

CONCLUSION

Studies performed by other investigators:

In addition, to the results reported above we implemented imaging protocols for different projects, including studies of aging, dementia, Parkinson's disease, GABA function, and primary HIV infection and the DOD pilot projects and funded described in the table below:

DAMD17-03-0532 Pilot Projects reviewed and selected during this period for funding:

Principal Investigator	Project Title	Project Status
Steven W. Cheung, M.D.	Repetitive Transcranial Magnetic Auditory Cortex Stimulation for Tinnitus Suppression	Pending Human Subjects Approval
Jialing Liu, Ph.D.	The Role of Corpus Callosum in Mediating Functional Recovery after Traumatic Brain Injury	Project start date: 9/16/05
Charles R. Marmar, M.D.	Cognitive Behavior Therapy and D-Cycloserine Treatment of PTSD in OEF and OIF Veterans	Project start date: 3/16/06
Dieter J. Meyerhoff, Dr. rer. Nat.	Brain GABA and Glutamate in Acute PTSD	Project start date: 6/1/06
Rajabrata Sarkar, M.D., Ph.D.	Matrix Metalloproteinase Therapy for Traumatic Limb Ischemia	Project start date: 9/16/05
Raymond A. Swanson, M.D.	Promoting Neurogenesis by Suppressing Microglia Activation	Project start date: 9/16/05

REPORTABLE OUTCOMES

Presentations:

Yu Zhang, PhD: Tractography-based and Voxel-Based studies of White Matter Changes in Normal Aging Using Diffusion Tensor Imaging on 4T. presented at: ISMRM

Antao Du, MD: Regional Decline of Brain cerebral Blood Flow in Healthy Aging by High-Field Arterial Spin Labeling; presented at: 58th American Academy of Neurology, San Diego, California.